Monografías Matemáticas *García de Galdeano* **43**, 41–50 (2024)

BAYESIAN MODELS FOR THE ANALYSIS OF CLIMATE CHANGE IN DAILY MAXIMUM TEMPERATURE SERIES

Alejandro Camón, Jorge Castillo-Mateo,
Jesús Asín and Ana C. Cebrián

Abstract. This paper proposes a Bayesian autoregressive model for daily maximum temperature series in the line of Castillo-Mateo et al. (J. Agric. Biol. Environ. Stat. 27, 3, 487–505, 2022). Here, the contribution is to consider the joint temporal modeling of the mean and variance of a Gaussian likelihood over 63 years in 18 temperature series located around Aragón, Spain. This model adopts two discrete temporal scales, year and day within year. For mean and variance it includes linear predictors like harmonic terms in days within years to capture seasonality, harmonic terms in interaction with a linear trend to capture seasonally-varying long-term trends, and interaction terms between the harmonics and the previous day's temperature to capture seasonally-varying persistence or serial correlation. The model is fitted using a Hamiltonian Monte Carlo algorithm with the Stan software, this algorithm returns posterior predictive samples to study the features of temperature of interest.

Keywords: autoregression, Bayesian model, Stan, time series, variance model.
AMS classification: 62F15, 62J05, 62M10, 62P12.

§1. Introduction

Climate change research is nowadays a hotspot [7], particularly in regards to estimating changes in temperature distribution or its mean [8]. To measure the variability of these changes, a statistical model for daily temperatures is necessary [10], specifically a model for daily maximum temperature (Tx).

With the rise of research on Bayesian modeling [1], models for Tx have been developed, taking into account temporal dynamics and potential relationships with other variables. Castillo-Mateo et al. [4] proposed a Bayesian spatio-temporal model for Tx during the warmest months of the year (from May to September). Their model includes a fixed effects component based on a linear trend in years, harmonic terms for the seasonal component, and an elevation term. It also includes an autoregressive term to capture persistence from the previous day's temperature, and random effects based on temporal and spatial Gaussian processes. A limitation of this model is that it assumes a constant variance over time for the daily local error term, which may not always be valid when working with the whole year.

This study aims to propose a new Bayesian model that can represent the distribution of Tx throughout the year. Overcoming some of the limitations of the model by Castillo-Mateo et al. is necessary, particularly by considering a submodel for the variance that depends on seasonal terms, persistence, or trends.

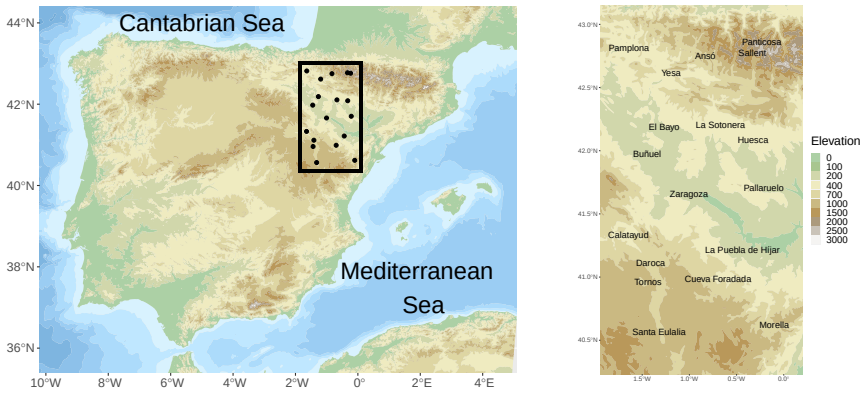

Figure 1: Location of the 18 stations in the Iberian Peninsula (left) and Aragón (right).

The outline of the paper is: Section 2 introduces the Tx data and develops an exploratory analysis, Section 3 proposes the joint model for mean and variance, Section 4 shows results of applying the model to the Tx data, and final conclusions are summarized in Section 5.

§2. Data and exploratory analysis

The analyzed database includes Tx from 18 Spanish stations around Aragón provided by AEMET, and it covers the period from 1953 to 2015. The elevation map shown in Figure 1 highlights the location of the 18 stations and the varied topography of the region. This region is known for its high climatic diversity due to its range of elevations and proximity to the Mediterranean and Cantabrian seas, as well as nearby mountain ranges. This variability poses a challenge for modeling daily temperatures, as noted by Castillo-Mateo et al. [4], especially considering the different patterns of temperature evolution in some areas of the region [8].

The exploratory analysis of the database reveals relevant characteristics that the proposed statistical model should include. Figure 2(a), showing boxplots of Tx by month in Zaragoza, confirms the seasonal behavior of temperatures. Similarly, Figure 2(b), showing the boxplots of temperature anomalies (defined as the difference between Tx and the average Tx for each day within year), highlights the seasonality of temperature variability, as indicated by the comparison of interquartile ranges.

Figure 2(c) represents the linear trend fitted to the annual mean temperature in Zaragoza and La Sotonera. The clearly different slopes across stations indicate the spatial diversity of the observed warming. Figure 2(c) also includes the linear trend fitted to the monthly mean temperature in June and September in Zaragoza to show the variability of the warming trend within the year.

Also persistence in Tx is a fundamental term. To avoid confusion with seasonality, we estimate the serial correlation on a monthly level at each station. For January data, the minimum first-order correlation across stations is 0.62, and the median is 0.70. For June, the corresponding values are 0.64 and 0.72, respectively.

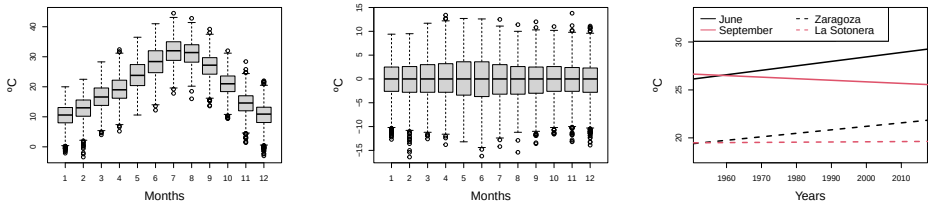

(a) Tx (b) Anomalies (c) Linear fits

Figure 2: Left and center: Boxplots of Tx by month in Zaragoza and its anomalies. Right: Fitted linear trend of the mean annual temperature (dashed) for La Sotonera (red) and Zaragoza (black), and linear trend of the mean monthly temperature (solid) for Zaragoza, June (black) and September (red).

Based on the results of the exploratory analysis, we have determined that our model should incorporate the following effects to accurately capture the temperature patterns with easily interpretable terms: i) a trend over the years to account for the impact of climate change, ii) the effect of persistence or the previous day's temperature to account for temperature inertia in the atmosphere, iii) the seasonal behavior of the mean temperature, the trend effect, and possibly the persistence, and iv) a non-constant variance over time.

§3. Modeling daily maximum temperature

In this work, we propose a new local model to capture the daily temperature evolution in each of the 18 stations separately. We augment our model with a submodel that accounts for the temporal variability of the Tx variance.

Let $Y_{t\ell}$ denote the daily maximum temperature on day ℓ, $\ell = 1, \ldots, L$ within year t, $t = 1, \ldots, T$. We assume that $Y_{t\ell}$ has a normal distribution conditioned on a set of covariates, $\mathbf{X}_{t\ell}$, including persistence, trend, and seasonality. The notation used for the mean and the variance submodels on day ℓ within year t are $\mu_{t\ell}$ and $\sigma^2_{t\ell}$, respectively. The first stage of the model is defined by $Y_{t\ell} = \mu_{t\ell} + \epsilon_{t\ell}$ with error term $\epsilon_{t\ell} \sim N(0, \sigma^2_{t\ell})$. Then, submodels for the mean and the variance are given by a mean-trend-autoregression structure as

$$\mu_{t\ell} = E[Y_{t\ell} \mid \mathbf{X}_{t\ell}] = \gamma_\ell + \phi_{t\ell} + \psi_{t\ell}, \quad \text{and} \quad \sigma^2_{t\ell} = Var[Y_{t\ell} \mid \mathbf{X}_{t\ell}] = \exp\{\gamma^\sigma_\ell + \phi^\sigma_{t\ell} + \psi^\sigma_{t\ell}\}, \quad (1)$$

where γ_ℓ and γ^σ_ℓ are independent terms expressed with harmonic terms—mean—, $\phi_{t\ell}$ and $\phi^\sigma_{t\ell}$ are long-term trends that interact with harmonics—trend—, and $\psi_{t\ell}$ and $\psi^\sigma_{t\ell}$ are autoregressive components that also interact with harmonics—autoregression. In particular,

$$\begin{aligned} \gamma_\ell &= \beta_0 + \sum_{i=1}^{N} \left(\beta_{i,s} Si_\ell + \beta_{i,c} Ci_\ell\right), \qquad \phi_{t\ell} = \left(\alpha_0 + \sum_{i=1}^{N_\alpha} \left(\alpha_{i,s} Si_\ell + \alpha_{i,c} Ci_\ell\right)\right) t, \\ \psi_{t\ell} &= \left(\rho_0 + \sum_{i=1}^{N_\rho} \left(\rho_{i,s} Si_\ell + \rho_{i,c} Ci_\ell\right)\right) Y_{t\ell-1}, \end{aligned} \quad (2)$$

with analogous structure for the variance but adding a superscript σ for notational purposes. For example, β_0 in the variance model is denoted by β_0^σ.

We make the following remarks:

- Days are indexed by $\ell = 1, \ldots, L$, where $L = 366$ for leap years and $L = 365$ otherwise.
- Year $t = 1$ corresponds to 1953 and $T = 63$ to 2015.
- For notational convenience, $Y_{t0} = Y_{t-1366}$ if $t - 1$ is a leap year and $Y_{t0} = Y_{t-1365}$ otherwise. Y_{11} is considered known.
- The harmonic terms are $Ci_\ell = \cos(2\pi i(\ell - 1)/366)$ and $Si_\ell = \sin(2\pi i(\ell - 1)/366)$.
- $N, N_\alpha, N_\rho, N^\sigma, N_\alpha^\sigma, N_\rho^\sigma$ are the number of harmonic functions used in each component of the submodels. These restrictions are imposed: $N_\alpha, N_\rho \leq N$ and $N_\alpha^\sigma, N_\rho^\sigma \leq N^\sigma$.
- The set of covariates is $\mathbf{X}_{t\ell} = (t, Y_{t\ell-1}, S1_\ell, C1_\ell, S2_\ell, C2_\ell, \ldots, SN_\ell, CN_\ell)$, with $N = max(N, N^\sigma)$.
- The vectors of parameters are:

$$\boldsymbol{\theta} = (\beta_0, \beta_{1,s}, \beta_{1,c}, \ldots, \beta_{N,s}, \beta_{N,c}, \alpha_0, \alpha_{1,s}, \alpha_{1,c}, \ldots, \alpha_{N_\alpha,s}, \alpha_{N_\alpha,c}, \rho_0, \rho_{1,s}, \rho_{1,c}, \ldots, \rho_{N_\rho,s}, \rho_{N_\rho,c}),$$
$$\boldsymbol{\theta}^\sigma = (\beta_0^\sigma, \beta_{1,s}^\sigma, \beta_{1,c}^\sigma, \ldots, \beta_{N^\sigma,s}^\sigma, \beta_{N^\sigma,c}^\sigma, \alpha_0^\sigma, \alpha_{1,s}^\sigma, \alpha_{1,c}^\sigma, \ldots, \alpha_{N_\alpha^\sigma,s}^\sigma, \alpha_{N_\alpha^\sigma,c}^\sigma, \rho_0^\sigma, \rho_{1,s}^\sigma, \rho_{1,c}^\sigma, \ldots, \rho_{N_\rho^\sigma,s}^\sigma, \rho_{N_\rho^\sigma,c}^\sigma).$$

3.1. Model fitting and residuals

Due to the complexity of the proposed Bayesian model, the use of Markov Chain Monte Carlo (MCMC) algorithms is necessary to obtain samples from the joint posterior distribution. More precisely, we use the Hamiltonian Monte Carlo (HMC) algorithm implemented in the package *RStan* [2, 9]. The HMC algorithm uses the derivatives of the density function being sampled to generate efficient transitions in the Markov chain to obtain the posterior distribution. This method uses simulations that exploit Hamiltonian dynamics in order to improve the acceptance rate of the Metropolis algorithm. The prior distribution considered for all parameters is a Gaussian and diffuse distribution, specifically a $N(0, 1000)$.

After fitting the models, we utilize the 95% credible intervals (CI95) to identify the covariates that are not significant. A covariate is deemed significant if the CI95 of its parameter does not contain zero.

We need to use a specific definition of residual in the validation analysis since the proposed approach models both the mean and the variance of the response. We define the residuals by standardizing the response with the posterior means of the mean and variance submodels, $\tilde{\mu}_{t\ell}$ and $\tilde{\sigma}_{t\ell}^2$, $e_{t\ell} = (y_{t\ell} - \tilde{\mu}_{t\ell})/\tilde{\sigma}_{t\ell}$. The proposed expression is based on the log-Gaussian density of the observation, which is adjusted to account for the non-stationary variance. Residuals obtained from this density are used to detect any issues in the fitted models.

§4. Results

This section provides a summary of the results. Firstly, we describe the procedure used to pre-select the number of terms in the model. Next, we present a summary of the model fitting, and finally, the final fitted model is used to characterize the changes in the distribution of Tx.

4.1. Pre-selection of covariates in the mean and variance submodels

To avoid overparameterization, variable selection is essential. To achieve this, a covariate-selection algorithm was developed, which compares non-Bayesian linear models for each station. Comparing multiple Bayesian models would have been computationally too expensive without a clear benefit.

In selecting the best mean submodel, our procedure aims to optimize the AIC criterion. We begin by including natural effects such as serial dependence and seasonality, and then analyze the effects of the trend. For seasonality, each harmonic component (sine and cosine with the same period) is gradually added until no improvement is found. To avoid overparameterization, we consider five nested models that sequentially explain most of the variability in the response: (i) Model *M*.0 uses only $Y_{t\ell-1}$, i.e. a simple AR(1) model; (ii) Model *M.har* adds harmonic terms to *M*.0; (iii) Model *M.har.int* introduces interactions between $Y_{t\ell-1}$ and harmonic terms; (iv) Model *M.trend* includes trend terms in addition to *M.har.int*; (v) Model *M.trend.int* adds interactions between harmonic terms and trend. The interactions in models *M.har.int* and *M.trend.int* allow us to model different persistence and trend effects for each day of the year. We compare the five fitted models and choose the one with the lowest AIC.

Inspired on the idea that $E[\epsilon_{t\ell}^2] = Var(\epsilon_{t\ell}) = \sigma_{t\ell}^2$, we implement the selection of the variance submodel. This is similar to the tools based on squared residuals that are used to detect heteroscedasticity. In this case, we apply the same procedure as above to the squared residuals from the fitted mean submodel. The fitting procedure identifies terms that show a systematic relationship with the expected value of the response, which is the residual variance.

The procedure for selecting the mean submodel is applied to each of the 18 stations, and in all cases, the resulting R^2 is higher than 0.83. Of the 18 stations, five have models without trend terms, with *M.har* selected in one station and *M.har.int* in four stations. Eleven stations have *M.trend* selected, and two stations have *M.trend.int* selected. All the mean submodels include at least two harmonic functions and the autoregressive term. Spatial patterns appear; for example, all the submodels without trend terms are in the north-west area. All the variance submodels include one harmonic function and the autoregressive term, with models without trend selected in six stations, *M.har* in three stations, *M.har.int* in three stations, *M.trend* in eight stations, and *M.trend.int* in four stations. No spatial patterns are observed regarding the variance submodels that include trend. The variance submodels have R^2 values around 0.05, which could be associated with the fact that daily variability is caused by the daily evolution of the atmospheric situation. Future work could improve the variance submodel by including atmospheric covariates.

4.2. Fitted models

To fit the models, two chains are simulated and 2,000 samples are saved from each. The chains are initialized with a warm-up period of 500 steps followed by a sampling period of 1,000 steps. If the resulting chains have not yet reached convergence, we increase the warm-up period to 9,000 steps to obtain 10,000 steps in total.

To evaluate the mixing of the model parameters, we followed usual criteria as suggested by Gelman et al. [6]. The potential scale reduction factor ($\hat{R}$) for all parameters was close to 1 and below 1.1, specifically ranging from 0.999 to 1.003. Additionally, the effective sample

Mean submodel			***Variance submodel***		
Parameter	Mean	CI 95%	***Parameter***	Mean	CI 95%
β_0	-160	$(-200, -120)$	β_0^σ	6.1	$(6, 6.2)$
$\beta_{1,s}$	-15	$(-17, -12)$	$\beta_{1,s}^\sigma$	*0.13*	$(-0.0039, 0.28)$
$\beta_{1,c}$	-34	$(-37, -31)$	$\beta_{1,c}^\sigma$	0.81	$(0.67, 0.94)$
$\beta_{2,s}$	6.8	$(5.9, 7.6)$	$\beta_{2,s}^\sigma$	-0.1	$(-0.15, -0.062)$
$\beta_{2,c}$	-1.2	$(-2, -0.32)$	$\beta_{2,c}^\sigma$	-0.05	$(-0.093, -0.0085)$
$\beta_{3,s}$	*0.001*	$(-0.53, 0.54)$	$\beta_{3,s}^\sigma$	*−0.015*	$(-0.042, 0.012)$
$\beta_{3,c}$	-1.2	$(-1.7, -0.67)$	$\beta_{3,c}^\sigma$	0.092	$(0.065, 0.12)$
α_0	0.11	$(0.094, 0.13)$			
ρ_0	0.68	$(0.67, 0.69)$	ρ_0^σ	0.0019	$(0.0015, 0.0023)$
$\rho_{1,s}$	0.03	$(0.018, 0.043)$	$\rho_{1,s}^\sigma$	*0.00025*	$(-0.00043, 0.00088)$
$\rho_{1,c}$	*0.0027*	$(-0.011, 0.016)$	$\rho_{1,c}^\sigma$	-0.0037	$(-0.0043, -0.0031)$

Table 1: Mean and credible interval of the posterior distribution of parameters in the model for Zaragoza. Non-significant terms appear in italics.

size for all but seven parameters was greater than 800, with the remaining seven having an effective sample size greater than 320.

Table 1 shows, as an example, a summary of the posterior distributions obtained for the parameters in the Bayesian model for Zaragoza. We found 18 significant terms and only four non-significant parameters, in italics, that are sine or cosine in some harmonic components where the other term is significant. The variance predictor uses seasonality terms and an autoregressive term.

Similar models are obtained for the other stations. The number of parameters in the 18 fitted models ranges from 13 (Yesa) to 26 (Pallaruelo). Almost all components in all of the models are significant, inducing that all of the proposed effects help to explain temperature distribution.

4.3. Estimating the warming over time

The fitted models enable us to evaluate the spatio-temporal variability of the trend effects, expressed in °C/decade and corresponding to a particular day ℓ within year. The trend is estimated using the posterior distribution of $\alpha_0 + \sum_{i=1}^{N_\alpha}(\alpha_{i,s}Si_\ell + \alpha_{i,c}Ci_\ell)$ in the mean submodel. Figure 3(a) shows the posterior densities of the trend in Tornos, Panticosa, and Zaragoza as illustration. In the Tornos model, a seasonal trend effect is included, as observed by the distinct posterior distributions in July 24 and December 24. A clearly positive trend is estimated in summer and a negative trend in winter, indicating that no common increasing effect is present throughout the year. In contrast, the Panticosa and Zaragoza models do not include interaction between the trend and seasonal terms. That is, the same positive trend is estimated within the year, with posterior medians of 0.05 and 0.11°C/decade, respectively.

Figures 3(b) and 3(c) show the posterior mean trend estimated on July 24 and December 24 for the mean submodel of Tx in the 18 stations. The maps were generated using a LOESS procedure, where the black line indicates zero trend, red represents higher values and yellow

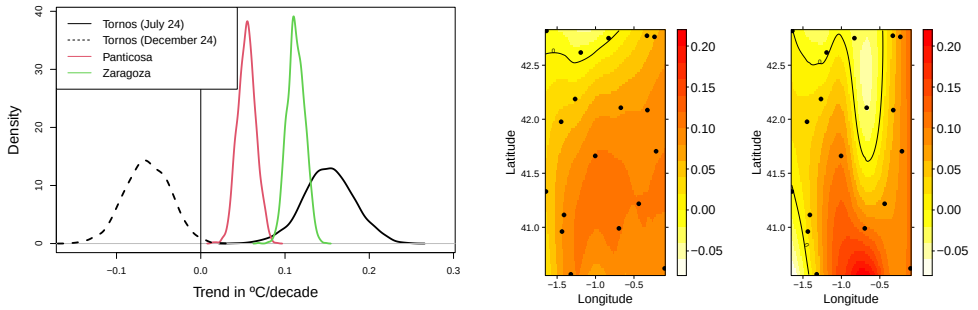

(a) Densities (b) July 24th (c) December 24th

Figure 3: Left: Posterior densities of the trend (°C/decade) in the mean of Tx, in Tornos (two different days), Zaragoza (non-seasonal) and Panticosa (non-seasonal). Center and right: Maps of the posterior mean of the estimated trend in the mean submodel in July 24 and December 24.

represents lower values. The spatio-temporal variability of the trend is evident, with a general increasing trend observed in summer, except in the north-west region. In winter, stations with a positive trend are also in the majority, although less than in summer. The spatial patterns observed in spring are similar to those in summer, and those in autumn are similar to winter.

Regarding the variance submodel, the trend effect has been found to be significant in 12 stations. However, it does not exhibit a clear pattern like the mean submodel. Seasonal behavior of the trend term has been observed only in a few stations, such as Santa Eulalia.

4.3.1. Estimation of the change in the marginal distribution

The Bayesian framework allows estimating the mean and quantiles of the marginal distribution of Tx. The posterior densities of the difference between monthly mean temperatures estimated in two decades 50 years apart (1955–1964 and 2005–2014) can be obtained. Figure 4 shows these densities in Zaragoza for January, June, and September. Despite the mean submodel not including seasonality in the trend effect, different warming rates are estimated in each month, likely due to other dynamic effects like persistence. June and September experienced a stronger warming than January, suggesting that the hottest period of the year is becoming longer.

4.4. Discussion

It is known that global warming effects are not the same in all climates and geographic regions [5]. The spatial heterogeneity in Aragón has also been identified by other authors. Peña-Angulo et al. [8] studied the evolution of the mean seasonal maximum and minimum temperatures in stations of the whole Iberian Peninsula between 1916 and 2015. They found an specially heterogeneous evolution with differences depending on the season: from 1956,

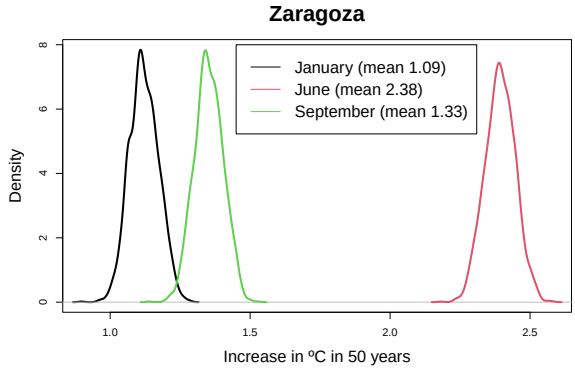

Figure 4: Posterior densities of the difference in mean Tx between 1955–1964 and 2005–2014, for January, June, and September in Zaragoza.

they estimate a trend of 0.31°C/decade in spring, 0.27°C/decade in summer, 0.13°C/decade in autumn and 0.17°C/decade in winter.

The spatial pattern found by Castillo-Mateo et al. [4] in their auto-correlation term ρ_0 are similar to the pattern in the posterior mean of the persistence effect during summer in our model. It is around 0.7, except in the north-west area, where a greater atmospheric variability appears. This similarity also appears in the spatial pattern of the warming in summer: they found that the posterior mean of the trend reaches greater values, near 0.35°C/decade, in the center of the Ebro Valley, while in the north-west the mean is close to zero.

Our methodology extends the work of Castillo-Mateo et al. by introducing a variance submodel that captures seasonal patterns and dependence on previous days in temperature variability. We also incorporate interaction terms with harmonics to model variations in persistence and trend effects within a year. Unlike prior studies, our model is fitted locally, which prevents overparameterization and permits a more informative analysis within each individual observed location. Although alternative approaches, such as quantile regression as proposed in [3], can analyze the evolution of variability, the assumption of independence across quantile levels makes it challenging to compare trends across quantiles jointly.

In contrast to our approach, a spatial model could offer several advantages over local models. Firstly, it permits the inclusion of geographical covariates such as elevation, which can improve the accuracy of the model. Secondly, it enables the analysis of global effects and the modeling of spatial dependence and patterns that may exist in the region, which can provide a more accurate and complete understanding of the underlying processes. Also, spatial modeling can provide more robust inference and prediction in areas where there are limited data, by borrowing strength from nearby locations. With the local models, we can produce maps to identify spatial patterns using interpolation of local results, however, we can not make inference on stations where registers do not exist. This can be done using spatial models such as the model by Castillo-Mateo et al.

§5. Conclusions

This work introduces a Bayesian autoregressive model that simultaneously models both the mean and the variance of the daily maximum temperature. One of the key advantages of this approach is the ability to incorporate seasonal effects using harmonic terms, as well as serial correlation, a long-term trend across years, and interaction terms between the seasonal component and other effects.

The model is fitted in a Bayesian framework based on the Hamiltonian Monte Carlo algorithm implemented in *RStan*. Given the complexity of the models, the algorithm is computationally expensive and leads to a slow convergence. For this reason, a model-selection procedure is implemented using a non-Bayesian approach as a preliminary step.

Models with the previous structure are fitted to each of 18 Tx series located around Aragón and measured from 1953 to 2015. All the fitted models include persistence and seasonal terms both in the mean and variance submodels. The trend terms in the mean submodel of the 18 stations allow us to identify spatial patterns of the evolution over time, in particular, an increasing trend in summer all over the region except in the northwest area. In all the variance submodels, several significant covariates are found, revealing the need for models including a time-varying variance. Using the previous fitted models, we can quantify the effect of global warming on temperature; for example, we estimate that, in Zaragoza, the mean of the increases of monthly mean temperature between decades 1955-1964 and 2005-2014 is higher than 1°C in January and September and higher than 2°C in June.

The structure of the model has many advantages. For example, it works on a daily scale so that any measure relates to the distribution of the daily temperature, but also any function of it such as means in different periods of time, can be studied using the model. Further, the model allows to generate simulated samples of Tx, so that it can be used as stochastic weather generator.

In our future work, we plan to evaluate the effectiveness of our models in representing extreme temperature data. Additionally, we aim to incorporate new atmospheric covariates that capture large-scale weather patterns. To achieve this, we will develop Bayesian spatial models and consider the use of Gaussian processes to account for spatial dependence not captured by covariates [4]. We will also explore the potential of the HMC algorithm for our models.

Acknowledgements

This work has been supported in part by the Grants PID2020-116873GB-I00 and TED2021-130702B-I00 funded by MCIN/AEI/10.13039/501100011033 and Unión Europea NextGenerationEU; and the Research Group E46_20R: Modelos Estocásticos funded by Gobierno de Aragón. J. C.-M. was supported by Gobierno de Aragón under Doctoral Scholarship ORDEN CUS/581/2020. The authors thank AEMET for providing the data.

References

[1] Banerjee, S., Carlin, B. P., and Gelfand, A. E. *Hierarchical Modeling and Analysis*

for Spatial Data, 2 ed. Chapman and Hall/CRC, New York, NY, USA, 2014. Available from: https://doi.org/10.1201/b17115.

[2] Carpenter, B., Gelman, A., Hoffman, M. D., Lee, D., Goodrich, B., Betancourt, M., Brubaker, M., Guo, J., Li, P., and Riddell, A. Stan: A probabilistic programming language. *Journal of Statistical Software 76*, 1 (2017).

[3] Castillo-Mateo, J., Asín, J., Cebrián, A. C., Gelfand, A. E., and Abaurrea, J. Spatial quantile autoregression for season within year daily maximum temperature data. *Annals of Applied Statistics* (in press). Available from: https://doi.org/10.1214/22-AOAS1719.

[4] Castillo-Mateo, J., Lafuente, M., Asín, J., Cebrián, A. C., Gelfand, A. E., and Abaurrea, J. Spatial modeling of day-within-year temperature time series: an examination of daily maximum temperatures in Aragón, Spain. *Journal of Agricultural, Biological and Environmental Statistics 27*, 3 (2022), 487–505.

[5] Fischer, E., Sippel, S., and Knutti, R. Increasing probability of record-shattering climate extremes. *Nature Climate Change 11*, 8 (2021), 689–695.

[6] Gelman, A., Carlin, J. B., Stern, H. S., Dunson, D. B., Vehtari, A., and Rubin, D. B. *Bayesian data analysis*. Chapman and Hall/CRC, 2013.

[7] IPCC. Global warming of 1.5°C. In *An IPCC Special Report on the impacts of global warming of 1.5°C above pre-industrial levels and related global greenhouse gas emission pathways*, V. Masson-Delmotte and et al., Eds. World Meteorological Organization, Geneva, Switzerland, 2018.

[8] Peña-Angulo, D., Gonzalez-Hidalgo, J. C., Sandonís, L., Beguería, S., Tomas-Burguera, M., López-Bustins, J. A., Lemus-Canovas, M., and Martin-Vide, J. Seasonal temperature trends on the Spanish mainland: A secular study (1916–2015). *International Journal of Climatology 41*, 5 (2021), 3071–3084.

[9] Stan Development Team. RStan: the R interface to Stan, 2022. R package version 2.21.7. Available from: https://mc-stan.org/.

[10] Verdin, A., Rajagopalan, B., Kleiber, W., Podestá, G., and Bert, F. BayGEN: A Bayesian space-time stochastic weather generator. *Water Resources Research 55*, 4 (2019), 2900–2915.

Alejandro Camón, Jorge Castillo-Mateo, Jesús Asín, Ana C. Cebrián
Department of Statistical Methods
University of Zaragoza
Pedro Cerbuna, 12
50009 Zaragoza, Spain
760371@unizar.es, jorgecm@unizar.es, jasin@unizar.es, acebrian@unizar.es